# Enhancing Low-Frequency Dynamic-Stiffness of Robotic Milling Machine Using Active Damping

Govind N. Sahu[1, *], Andreas Otto[1] and Steffen Ihlenfeldt[1]

[1] Fraunhofer Institute for Machine Tools and Forming Technology, IWU, Chemnitz, Saxony, 09126, Germany
* Department of Mechanical Engineering, Indian Institute of Technology Tirupati, Tirupati, Andhra Pradesh, 517619, India
govinds@iittp.ac.in

**Abstract.** Industrial robots have gained prominence due to their large workspace and cost-effectiveness. However, their limited static and dynamic compliance restricts their machining capabilities across various materials. Particularly, the inadequate dynamic stiffness of milling robots results in detrimental phenomena like mode coupling chatter and regenerative chatter, even at shallow cutting depths. These issues detrimentally impact performance, product quality, tool, and may even induce damage to robot components. This study focuses on addressing the challenge of low dynamic stiffness in milling robots by employing active damping. The active control system employs an acceleration sensor to detect vibrations in real-time and an actuator to counteract undesirable oscillations based on the controlled signal. However, the actuator's inherent natural frequencies often align with the robot's structural modes, limiting its efficacy in damping low-frequency vibrations. To overcome this, a compensator is proposed utilizing pole-placement techniques, effectively suppressing actuator-related modes, and enhancing suitability for attenuating low-frequency vibrations. Experimental results reveal a substantial enhancement of up to ~103% in robot dynamic stiffness because stiffness is increased by ~103% at the natural frequency of the robot. This improvement proportionately increases the stability limit and enables chatter-free material removal, consequently elevating the overall performance of the robotic milling system. This advancement holds promise for expanding the capabilities of industrial robots in various machining applications.

**Keywords:** Active damping, Machining, Chatter, Robotic milling.

## 1 Introduction

Industrial robotics has gained immense popularity owing to its substantial workspace flexibility, cost-effectiveness, reduced setup time, and has thus found increasing demand in the milling of large, lightweight aerospace components. Despite these advantages, robots exhibit lower static and dynamic stiffness compared to conventional machine tools, limiting their suitability for various machining processes [1]. The deficiency in dynamic stiffness of robotic milling systems leads to the occurrence of regenerative chatter even at minimal depths of cut, consequently hampering productivity, compromising product quality, and potentially causing tool wear or machine damage [1–4]. Moreover, the existence of identical eigenfrequencies in the two principal directions of the robot instigates mode coupling chatter, resulting in unstable robotic milling processes [4,5]. To surmount these challenges, this study employs active damping systems to counteract vibrations and enhance the overall performance of robotic milling.

Active damping systems incorporate sensors to detect vibrations in real-time and actuators to apply controlled forces that counter undesired oscillations. By actively dampening vibrations, the stability of the milling process can be significantly improved, thereby leading to superior surface finishes [6–8]. These systems leverage advanced control algorithms to adaptively respond to dynamic changes within the system [8]. Furthermore, the robotic milling machine comprises both low and high-frequency modes. The low-frequency structural modes of the robot are dependent on its pose, whereas the high-frequency modes are attributed to the milling spindle and cutting tool combination, remaining unchanged as the robot's tool position changes [2,7]. The pose-dependent low-frequency modes become unstable due to regenerative chatter and self-excited mode coupling chatter, especially during low-speed cutting of high-strength or thermally resistant materials [2]. On the other hand, the high-frequency modes of the robotic milling system destabilize when cutting lightweight materials at high spindle speeds [2].

Prior research has extensively explored aspects of the robotic milling system, encompassing stability analysis [2,3,8,9], robot pose optimization [10], active chatter control in robotic milling [7–9], enhancement of positional accuracy [11], and identification and modeling of pose-dependent robot dynamics [10]. However, despite advancements in understanding milling chatter and improving robotic milling stability, a significant gap remains in the literature regarding the enhancement of dynamic stiffness within low-frequency robot structural modes. This research addresses this gap by introducing an active inertial actuator affixed to the robotic milling head to enhance the dynamic stiffness of these low-frequency structural modes.

It's noteworthy that many inertial actuators available in the market and integrated into industrial robots possess eigenfrequencies ranging from 5 to 30 Hz [6,12,13]. Implementing active damping using such active inertial actuators for robotic milling performance enhancement is not a straightforward undertaking, as resonances between the robot's modes and the actuator's modes can potentially amplify vibrations instead of mitigating them. Analogous issues concerning low-frequency vibrations arise in gantry-type portal milling machines [14]. To address these challenges, a common approach involves designing an actuator compensator that reduces the magnitude of the actuator's mode. Bilbao-Guillerna et al. have proposed various compensatory filter variations to expand the linear range of inertial actuators and enhance milling stability in ram-type portal milling machines [15]. Nonetheless, these compensator filters often exhibit significant magnitudes at very low frequencies, including up to 5 Hz, potentially amplifying low-frequency signals and compromising active damping robustness. Consequently, this study also introduces a compensator filter design that effectively suppresses the actuator mode without inducing instability, thereby ensuring that very low-frequency modes are not subject to amplification.

The subsequent sections of the paper are structured as follows: Section 2 elucidates the outcomes of the experimental modal analysis conducted on the robot, along with the dynamic characterization of the actuator. The design methodology for the compensation filter and the selection of additional filter parameters are illustrated in Section 3. To facilitate the active damping experiments and ascertain the closed-loop system's stability, a Simulink model has been developed, as described in Section 4. Section 5 encapsulates the results of the experimental modal analysis performed on the robotic milling system featuring active damping. Finally, the summary of the paper is presented in the Conclusions section.

## 2 Characterization of Robot and Actuator Dynamics

The robotic milling system, which includes an inertial actuator (Make: Micromega Dynamics, Model: ADD45) attached to the milling spindle head, is depicted in Fig. 1(a). Through initial modal experiments, we determined that the robot is most flexible in the Y direction. Thus, for this study, we positioned the actuator horizontally in the Y direction. We employed a standard end mill cutter with a 10 mm diameter and two teeth. In this setup, the tool center point (TCP) is marked as location 1, while location 2 indicates the actuator mounting location (AML). The actuator was firmly secured using screws. To capture vibrations and provide feedback, a tri-axial accelerometer (Make: PCB, Model: JTLB356B08) was strategically placed near location 2. We specifically used the acceleration signal in the Y direction for feedback purposes. The accelerometer's signal was then sent to the controller for further analysis and monitoring of the system.

### 2.1 Modal Analysis of the Robot Without Active Damping

Modal experiments were conducted using an impact hammer (Make: Dytran, Model: 5800B4), a tri-axial accelerometer, and the MalTF module of CutPro software. All the modal experiments were conducted using the actuator mount (see Fig. 1(a)), as it will be attached during active damping tests. In Fig. 1(b), the notation $H_{21yy}$ represents the Cross-Frequency Response Function, FRF of the robot and the tool holder-tool arrangement. Here, location 1 serves as the excitation point, while measurements occur at location 2, with both directions aligned along the Y axis. Lower frequency modes are associated with the robot's structure [2,7]. To capture these modes at the tool tip, a tri-axial accelerometer was magnetically attached near the tool's shank within the tool holder. This accelerometer measured FRFs directly at the tool tip, designated as ($H_{11xx}$, $H_{11yy}$, and $H_{11zz}$). As the actuator is mounted in the Y direction, measurements of the direct and cross FRFs at the AML were solely taken in the Y direction, focusing on understanding the actuator's impact on the system's response in the Y direction, as illustrated in Fig. 1(b).

(a)

(b)

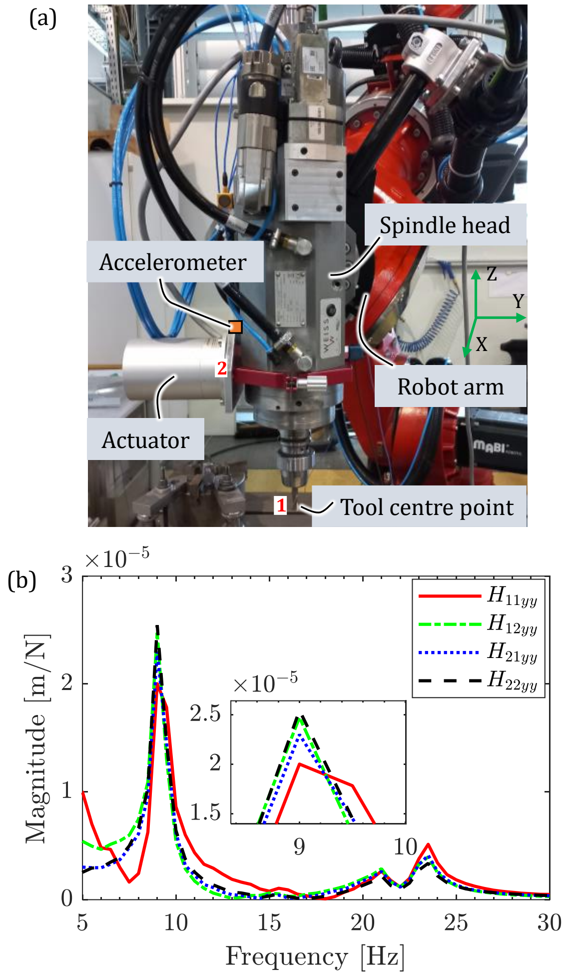


**Fig. 1.** (a) A robotic milling setup with actuator mount, (b) Measured direct and cross FRFs of robot millling system in Y direction.

### 2.2 Characterization of the Actuator

The actuator's characterization was conducted using the setup shown in Fig. 2(a). To ensure precise force measurements, the actuator was mounted on the Kistler Dynamometer (Model: 9255B, SN: 485906). As the robot's configuration varies based on its usage, our study focused on testing the actuator solely in horizontal orientations. Using a LabVIEW code, we generated a sine chirp signal at 1 Voltage, spanning from 1 Hz to 200 Hz. This broad frequency range enabled a comprehensive assessment of the actuator's performance across various frequencies. To facilitate data collection and transmission, we employed a Compact RIO controller (Model: NI cRIO 9047), which incorporated an analog-to-digital converter (Model: NI 9232) to receive force signals from the Kistler dynamometer. Simultaneously, a digital-to-analog converter (Model: NI 9263) was utilized alongside a power amplifier to transmit voltage signals to the actuator. The collected time-domain input voltage and output force signals were then transformed into the frequency domain using FFT (Fast Fourier Transform), as demonstrated in Fig. 2(b).

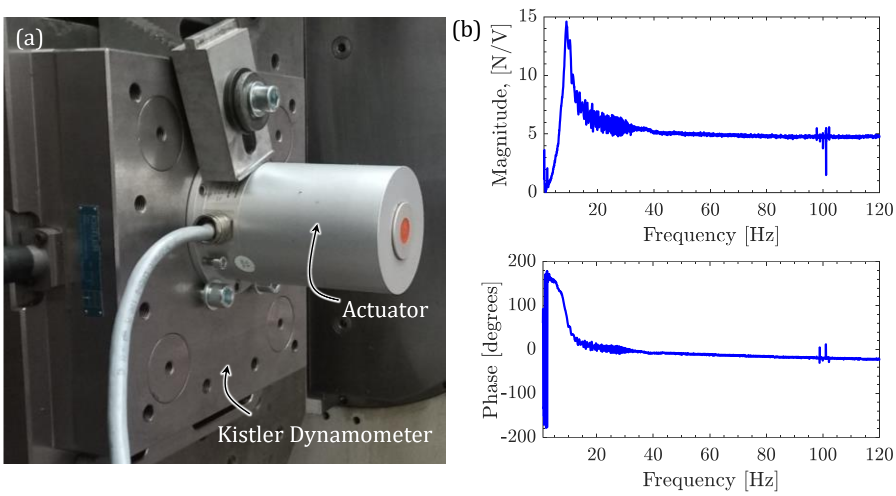


**Fig. 2.** (a) Actuator mounted horizontally on the Kistler dynamometer (b) Estimated force-voltage-frequency characteristics of the actuator.

Fig. 2(b) shows that the actuator's natural frequency is 9 Hz, which is similar to the robot's natural frequency of 9.2 Hz (see Fig. 1(b)). This proximity raises concerns about resonance that could amplify the robot's vibrations. Due to this resonance issue, the actuator cannot be directly utilized for active damping. To address this challenge, the following section outlines the design of a compensation filter. This filter aims to enable effective use of the actuator at lower frequencies by mitigating the resonance effect and flattening the actuator's response, making it suitable for active damping purposes..

## 3 Design of Compensation Filter for Actuator

The compensation filter for the actuator is designed with specific goals: (i) to reduce the effect of the actuator's behavior, aiming to even out its response specially near the eigen frequency of the actuator, (ii) to ensure that the filter has minimal or unity magnitude at zero frequency, and (iii) to maintain stability by placing the filter's poles on the left side of the complex plane. Directly inverting the actuator's FRF or its mathematical representation leads to instability and exaggerated behavior at zero frequency. Thus, this study employs a strategic approach: it selects the positions of poles and zeros to achieve the desired reduction in the actuator's influence while maintaining overall stability. To begin, the MATLAB Control System Designer Toolbox is used to approximate the FRF of the actuator, based on the data shown in Fig. 2(b). This approximation follows the three criteria mentioned earlier. The resulting actuator transfer function is given below:

$$G_{\mathrm{act}}(s) = \frac{1.612\, s^3 + 1278\, s^2 + 7.733e04\, s + 1.453e05}{s^3 + 174.6\, s^2 + 8221\, s + 5.491e04} \tag{1}$$

The frequency response of $G_{\mathrm{act}}(s)$ is depicted in Fig. 3(a). As Eq. (1) exhibits nonminimum phase behavior, direct inversion is not viable[16] because inverted version of Eq. (1) will have poles on the right side of the complex plane, indicating an unstable system [16]. To overcome this, we employed MATLAB's *invfreqz* function with a sampling rate of 5 ms, facilitating the transformation of the transfer function into a minimum phase form [16]. This transformation involves minimizing the weighted sum of squared errors between the actual transfer function's absolute magnitudes and the polynomial ratio, evaluated at different frequencies. An inverted version of $G_{\mathrm{act}}(s)$ with minimum phase system, i.e. a stable compensation filter transfer function is given below:

$$C(s) = \frac{3\, s^3 + 413.7\, s^2 + 17241\, s + 211110}{1.004\, s^3 + 1254\, s^2 + 98360\, s + 186300} \tag{2}$$

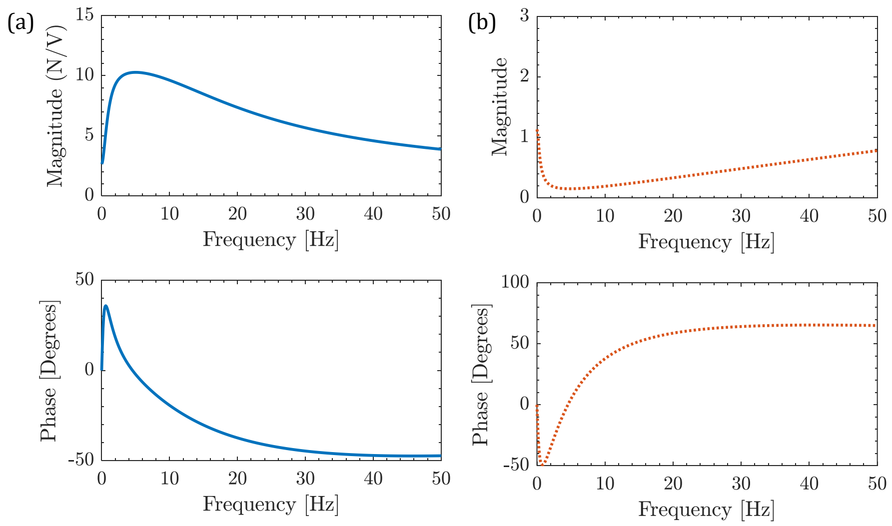


**Fig. 3.** (a) Approximated actuator dynamics (b) Designed compensator dynamics.

The results in Fig. 3(a) show that the actuator dynamics are closely approximated in terms of magnitude, though this comes with a compromise in the phase diagram. The frequency responses of the compensation filter, $C(s)$ is presented in Fig. 3(b), which makes it evident that the bode plot's magnitude remains notably low for frequencies under 20 Hz and influences nearby frequencies. These filter characteristics were integrated into a multi-input-multi-output (MIMO) closed-loop active damping model before real experiments, as detailed in the subsequent section.

## 4 Modelling of Closed-loop Active Damping System

To assess the effectiveness of the control strategy, a Simulink model utilizing a multi-input multi-output (MIMO) configuration has been developed, as illustrated in Fig. 4. In this model, the direct and cross FRFs of the robotic milling system have been selected specifically for the Y direction, as the actuator is mounted in that direction, yielding the most significant impact. Notably, the receptance FRFs (x/F) have been utilized in the Simulink model to obtain the displacement signal as an output. Consequently, a differentiator ($s$) has been employed to derive the velocity signal from the displacement signal, which serves as a feedback signal to the controller. This strategy is commonly known as direct velocity feedback (DVF) technique, which has been widely used for suppressing chatter in machining [8,12,17].

Given the actuator's maximum force capacity of 45 N, we integrated a force saturation block at 36 N (~9 Volts), depicted in Fig. 4. To address inherent vibrations resulting from the robot's position control loop at 3 Hz, we introduced a 3 Hz sine wave with white noise signal to the acceleration signal. Filters were integrated into the feedback signal, including a notch filter to eliminate the 3 Hz signal, a high-pass filter to eliminate noise/vibrations below the robot's natural frequency, and a low-pass filter eliminating high-frequency noise.

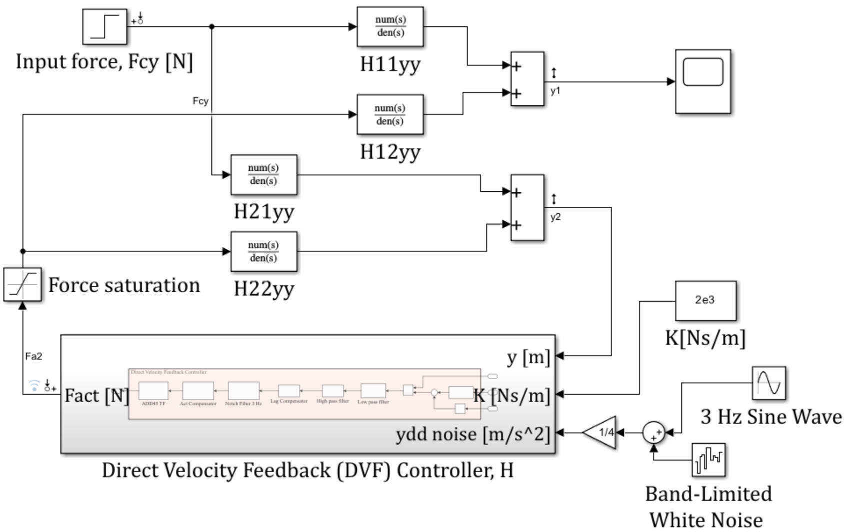


**Fig. 4.** Simulink model of the closed-loop active damping system.

Preliminary theoretical exploration indicated that the closed-loop system exhibited substantial phase lead due to the high-pass filter (second order, cut-off frequency – 4 Hz), the notch filter (second order, center frequency – 3 Hz), and the compensation filter. To counteract this phase lead, we decreased the low-pass filter's cut-off frequency to 50 Hz and applied it twice. This approach ensured that the negative phase contribution provided by the low-pass filter compensated for the overall phase lead in the closed-loop system. The filter parameters were implemented using LabVIEW software. The direct velocity feedback controller (DVF), denoted as $H(s)$ in Fig. 4, is defined as follows:

$$H(s) = sK\ G_{\mathrm{lpf}}(s)G_{\mathrm{lpf}}(s)\ G_{\mathrm{hpf}}(s)\ G_{\mathrm{notch}}(s)\ G_{\mathrm{act}}(s)C(s) \tag{3}$$

Where, $K$ (Ns/m) is the closed loop control gain. The transfer function of the closed-loop control system when feedback is taken from location 2 is given by:

$$\frac{y_1}{F_{cy}}(s) = \frac{H_{11yy}\left(1+\frac{H}{T}\right)-H_{12yy}\,H_{21yy}\,H}{1+\frac{HH_{22yy}}{T}} \tag{4}$$

Since roots of the denominator of the closed-loop transfer function governs the closed-loop stability, denominator of Eq. (4) has been extracted as given below:

$$1+\frac{HH_{22yy}}{T} = 0 \tag{5}$$

$$1+GH = 0 \tag{6}$$

wherein, $G = H_{22yy}/T$. Using $GH$ from Eq. (6), stability of the closed-loop system has been checked using a root locus technique, correspondingly active damping experiments are conducted within the stable control gain limit, as described in the subsequent section.

## 5 Modal Analysis of the Robot with Active Damping

The schematic diagram illustrating the closed-loop active damping system of the robotic milling machine is presented in Fig. 5. As mentioned in the last section, a well-established non-model-based direct velocity feedback (DVF) control law was utilized [6,8,12,17]. In experiments, since we have used an accelerometer, an integrator has been used to get the velocity signal and complete the DVF strategy. The same number of filters as mentioned in Fig. 4 and Eq. (3) have been implemented in the LabVIEW software, which works as a digital controller. For the control system, a Compact RIO controller based on FPGA program (Make: National Instrument, Model: cRIO9047) was employed. This controller is equipped with analog-to-digital (ADC, Model: NI9225) and digital-to-analog converter (DAC, Model: NI9263) modules, which support IEPE (Integrated Electronic Piezoelectric) functionality. The controller is connected to a PC, where LabVIEW software is utilized to manage and regulate the actuator. In the present work, the experimental implementation of active damping was done as suggested in Ref. [17].

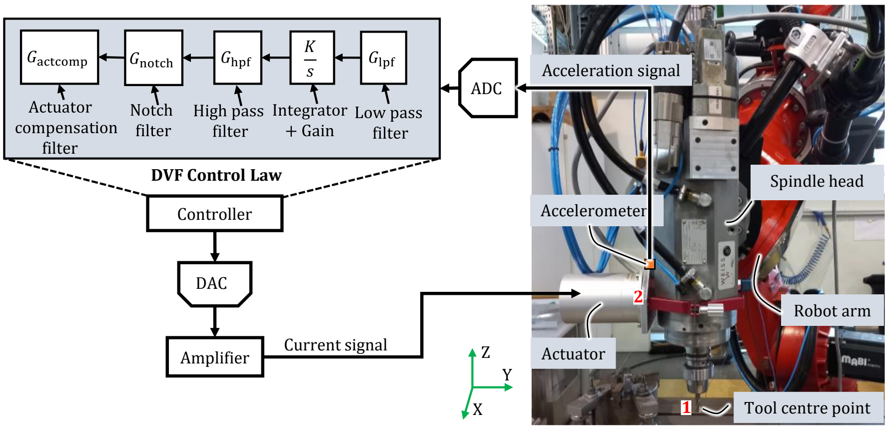


**Fig. 5.** Robotic milling system with integrated active inertial actuator.

For modal analysis of a robotic milling machine with active damping, we first switch On the controller with a desired control gain and then perform the impact test, similar way as described in Section 2.1 After preliminary experimental investigation on effect of active damping on $H_{22yy}$, we found a suitable value of control gain ($K = 2000\ \text{Ns/m}$) that is stable and gives maximum improvement in dynamic stiffness, therefore, this value of control gain has been used in other experiments.

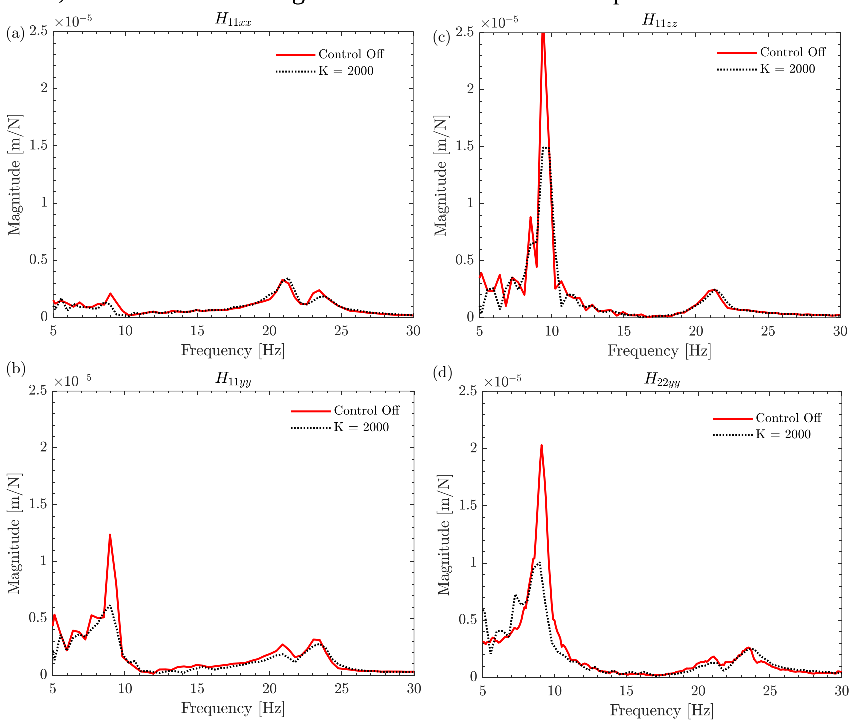


**Fig. 6.** Direct FRFs at the TCP and cross FRF between tool tip and AML with active control Off and On.

Since dynamics of the tool in all three orthogonal directions (X, Y and Z) directly affect the minimum stability of the machining process, direct FRFs ($H_{11xx}$, $H_{11yy}$ and $H_{11zz}$) at the TCP are measured with active damping being On, results of which are shown in Fig. 6. It is noted that the robot is most stiff in X direction because robot structures are aligned in that direction (see Fig. 5). Furthermore, robot Y and Z direction is the most flexible as it is perpendicular to the X axis and not much structural support is there. However, the stiffness of the robot can be changed depending on upon the position and orientation of the robot.

Fig. 6 clearly demonstrates that with proper selection of filters, control parameters, and control strategy, it effectively suppresses the robot's structural mode, resulting in maximum 103.2% improvement in dynamic stiffness. The maximum improvement in dynamic stiffness of the robotic milling machine at the natural frequency of the robot (9.2 Hz) in X, Y and Z directions are listed in Table 1. This also means an improvement in depth of cut and material removal rate of ~103%. Since the actuator is mounted in the Y direction, active damping is most effective in the same direction, resulting in a maximum improvement in dynamic stiffness of ~103% at the actuator mounting location and ~101% at TCP. It is also noted that effect of active damping force at location 2 in Y direction also suppresses the peaks in X, Y and Z directions at the TCP.

**Table 1.** Percentage improvement in dynamic stiffness of the robot at its natural frequency (9.2 Hz).

| FRFs | $H_{11xx}$ | $H_{11yy}$ | $H_{11zz}$ | $H_{22yy}$ |
|---|---|---|---|---|
| Improvement | 91.25% | 100.91% | 79.30% | 103.20% |

## 6 Conclusions

In this paper, the challenges posed by lower dynamic compliance of industrial robots in comparison to conventional machine tools for milling applications were addressed. The deficiencies in dynamic stiffness lead to issues like regenerative chatter and mode coupling chatter, impacting machining productivity, product quality, and tool wear. To overcome these challenges, the study introduced an active damping system that employs sensors and actuators to counteract vibrations, enhancing the overall performance of robotic milling. The paper presented a comprehensive investigation, including the experimental modal analysis of the robot and actuator dynamics. The actuator's characteristics were carefully examined, revealing its natural frequency close to the robot's natural frequency, which could lead to resonance issues. To mitigate this problem, a compensation filter design was introduced to attenuate the actuator mode while maintaining stability. This filter was designed through MATLAB and transformed into a minimum phase form to ensure stability.

The study developed a closed-loop active damping system model in Simulink, utilizing a direct velocity feedback control strategy. The system's stability was analyzed using root locus techniques, ensuring safe experimentation. The active damping system was integrated into the robotic milling machine, and experiments were conducted to assess its effectiveness. The results demonstrated significant improvements in dynamic stiffness of the robot at its natural frequency, with a maximum enhancement of approximately 103% in the Y direction. This improvement of dynamic stiffness led to proportionately ~103% improvement in depth of cut and material removal rate.

In conclusion, the paper successfully tackled the challenge of enhancing dynamic stiffness within low-frequency robot structural modes for robotic milling applications. The proposed active damping system, along with the compensation filter, effectively addressed resonance issues, leading to improved stability and productivity in robotic milling processes. This research contributes to bridging the gap in the literature related to dynamic stiffness enhancement in robotic milling systems, paving the way for more efficient and precise machining of aerospace components and other industries. As a future direction, the study plans to expand its scope by exploring the utilization of multiple actuators and their synchronization within the active control strategy during machining experiments.

## References

[1] Verl A, Valente A, Melkote S, Brecher C, Ozturk E, Tunc LT. Robots in machining. CIRP Annals 2019;68:799–822. https://doi.org/10.1016/j.cirp.2019.05.009.

[2] Cordes M, Hintze W, Altintas Y. Chatter stability in robotic milling. Robot Comput Integr Manuf 2019;55:11–8. https://doi.org/10.1016/j.rcim.2018.07.004.

[3] Xin S, Peng F, Tang X, Yan R, Li Z, Wu J. Research on the influence of robot structural mode on regenerative chatter in milling and analysis of stability boundary improvement domain. Int J Mach Tools Manuf 2022;179. https://doi.org/10.1016/j.ijmachtools.2022.103918.

[4] Yuan L, Pan Z, Ding D, Sun S, Li W. A Review on Chatter in Robotic Machining Process Regarding Both Regenerative and Mode Coupling Mechanism. IEEE/ASME Transactions on Mechatronics 2018;23:2240–51. https://doi.org/10.1109/TMECH.2018.2864652.

[5] Cen L, Melkote SN. CCT-based mode coupling chatter avoidance in robotic milling. J Manuf Process 2017;29:50–61. https://doi.org/10.1016/j.jmapro.2017.06.010.

[6] Sahu GN, Deora P, Law M, Wahi P. Adaptive model-free gain tuning for active damping of machine tool vibrations. Journal of Vibration Engineering & Technologies 2022;10:2799–808. https://doi.org/https://doi.org/10.1007/s42417-022-00520-0.

[7] Nguyen V, Johnson J, Melkote S. Active vibration suppression in robotic milling using optimal control. Int J Mach Tools Manuf 2020;152. https://doi.org/10.1016/j.ijmachtools.2020.103541.

[8] Ozsoy M, Sims ND, Ozturk E. Robotically assisted active vibration control in milling: A feasibility study. Mech Syst Signal Process 2022;177. https://doi.org/10.1016/j.ymssp.2022.109152.

[9] Guo K, Zhang Y, Sun J. Towards stable milling: Principle and application of active contact robotic milling. Int J Mach Tools Manuf 2022;182. https://doi.org/10.1016/j.ijmachtools.2022.103952.

[10] Cvitanic T, Nguyen V, Melkote SN. Pose optimization in robotic machining using static and dynamic stiffness models. Robot Comput Integr Manuf 2020;66. https://doi.org/10.1016/j.rcim.2020.101992.

[11] Cen L, Melkote SN, Castle J, Appelman H. A Wireless Force-Sensing and Model-Based Approach for Enhancement of Machining Accuracy in Robotic Milling. IEEE/ASME Transactions on Mechatronics 2016;21:2227–35. https://doi.org/10.1109/TMECH.2016.2567319.

[12] Sahu GN, Vashisht S, Wahi P, Law M. Validation of a hardware-in-the-loop simulator for investigating and actively damping regenerative chatter in orthogonal cutting. CIRP J Manuf Sci Technol 2020;29:115–29. https://doi.org/10.1016/j.cirpj.2020.03.002.

[13] Operation and maintenance manual, 45N active damping devices , MICROMEGA DYNAMICS. 2017.

[14] Abele E, Pfeiffer G, Jalizi B, Bretz A. Simulation and development of an active damper with robust μ-control for a machine tool with a gantry portal. Production Engineering 2016;10:519–28. https://doi.org/10.1007/s11740-016-0691-6.

[15] Bilbao-Guillerna A, Azpeitia I, Luyckx S, Loix N, Munoa J. Low Fre-quency Chatter Suppression using an Inertial Actuator. 2012.

[16] Magnevall M, Lundblad M, Ahlin K, Broman G. High frequency measurements of cutting forces in milling by inverse filtering. Machining Science and Technology 2012;16:487–500. https://doi.org/10.1080/10910344.2012.698970.

[17] Sahu N, Law M. Hardware-in-the-loop simulator for emulation and active control of chatter n.d. https://doi.org/10.17605/OSF.IO/8N47G.

## Acknowledgement

The first author of this paper would like to express sincere gratitude for the support received from the IGSTC Post-Doctoral Industrial Fellowship (PDIF) – 2021. The research presented in this paper was conducted exclusively at the Fraunhofer Institute for Machine Tools and Forming Technology, IWU, Germany.